# Supporting Information Appendix for

## The Mechanism of Burgess Shale-type Preservation

Robert. R. Gaines[a*1] Emma U. Hammarlund[b,c,d*], Xianguang Hou[e], Changshi Qi[e], Sarah E. Gabbott[f], Yuanlong Zhao[g], Jin Peng[g] and Donald E. Canfield[b]

[a]Geology Department, Pomona College, Claremont, CA 91711, USA; [b]Nordic Center for Earth Evolution, DK-5230 Odense M, Denmark; [c]Department of Palaeozoology, Swedish Museum of Natural History, SE-104 05 Stockholm, Sweden; [d]Department of Geosciences, Stockholm University, SE-106 91 Stockholm, Sweden; [e]Yunnan Key Laboratory for Palaeobiology, Yunnan University, Kunming 650091, China; [f]Department of Geology, University of Leicester, University Road, Leicester LE1 7RH, UK and [g]Key Laboratory for Paleobiology, Guizhou University, Guiyang, China

[*]These two authors contributed equally to this work and are listed alphabetically.

[1] To whom correspondence should be addressed. E-mail: robert.gaines@pomona.edu.

**This PDF includes**

Supporting figures S1 to S8
Supporting tables S1-S2
References

## Supporting figures and captions

Figure S1: Stratigraphic positions of sampled units
Figure S2: Microfabrics of BST claystones
Figure S3: Carbonate cements in BST claystones
Figure S4: Elemental maps of BST claystone beds
Figure S5: $\delta^{13}C$ vs. $\delta^{18}O$ of carbonate cements from Haikou core (Chengjiang)
Figure S6: $\delta^{34}S$ across single BST event beds
Figure S7: $\delta^{34}S$ vs. bed thickness
Figure S8: Event bed pyrite concentration vs. time

## Supporting tables

Table S1. The isotopic composition of sulfur pyrite in Chengjiang and 6 other principal Burgess shale type deposits.
Table S2. $\delta^{13}C$ vs. $\delta^{18}O$ of carbonate cements from BST-bearing claystones

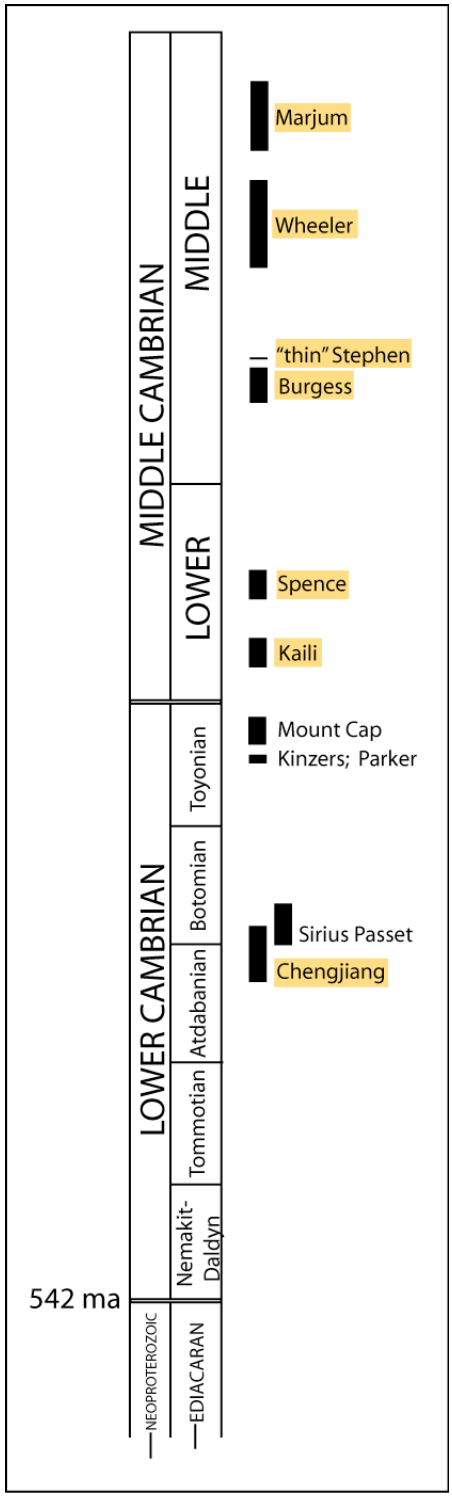


**Figure S1**: Stratigraphic distribution of the principal Burgess Shale-type deposits across Lower (Series 2) and Middle (Series 3) Cambrian strata, modified from Conway Morris (1). Deposits analyzed in this study are highlighted in yellow. The recently- reported BST locality in the "thin" Stephen Formation of British Columbia (2) as not among the principal BST deposits identified by Conway Morris (1). Among these deposits, the Chengjiang and Burgess Shale are, by far, the most important in diversity and abundance of soft-bodied fossil biotas that they have yielded (3, 4). Mount Cap is known only from the subsurface (5), and Kinzers/Parker and Sirius Passet have experienced extensive metamorphism (e.g. (6, 7)).

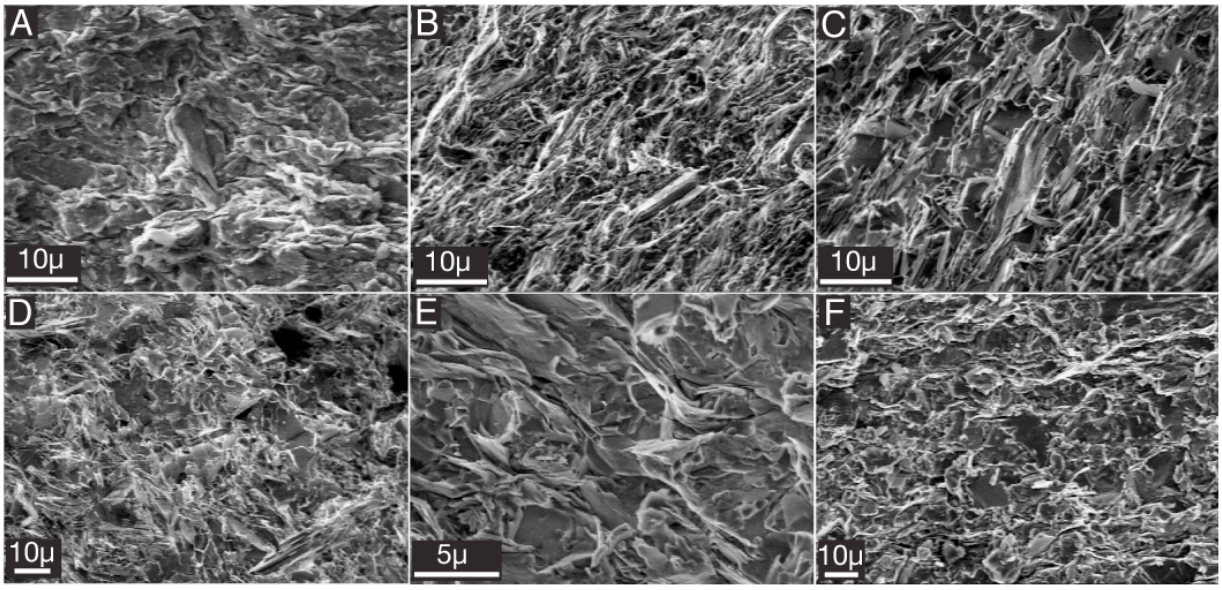


**Figure S2:** SEM micrographs showing BST claystone microfabrics from the Chengjiang (A), Kaili Fm. (B), Spence Shale Mbr. (C), "thin" Stephen Fm. (D), Wheeler Fm. (E) and Marjum Fm. (F). All surfaces analyzed were freshly broken perpendicular to bedding. In all cases BST-bearing claystones exhibit randomly-oriented clay-microfabrics, indicative of rapid deposition from turbid suspension by bottom flowing currents (8). These images also demonstrate the predominance of clay minerals and the absence of silt or coarser-grained particles from the BST facies of all deposits. An SEM micrograph of clay fabric from the Walcott Quarry Member of the Burgess Shale is shown in Figure 2A.

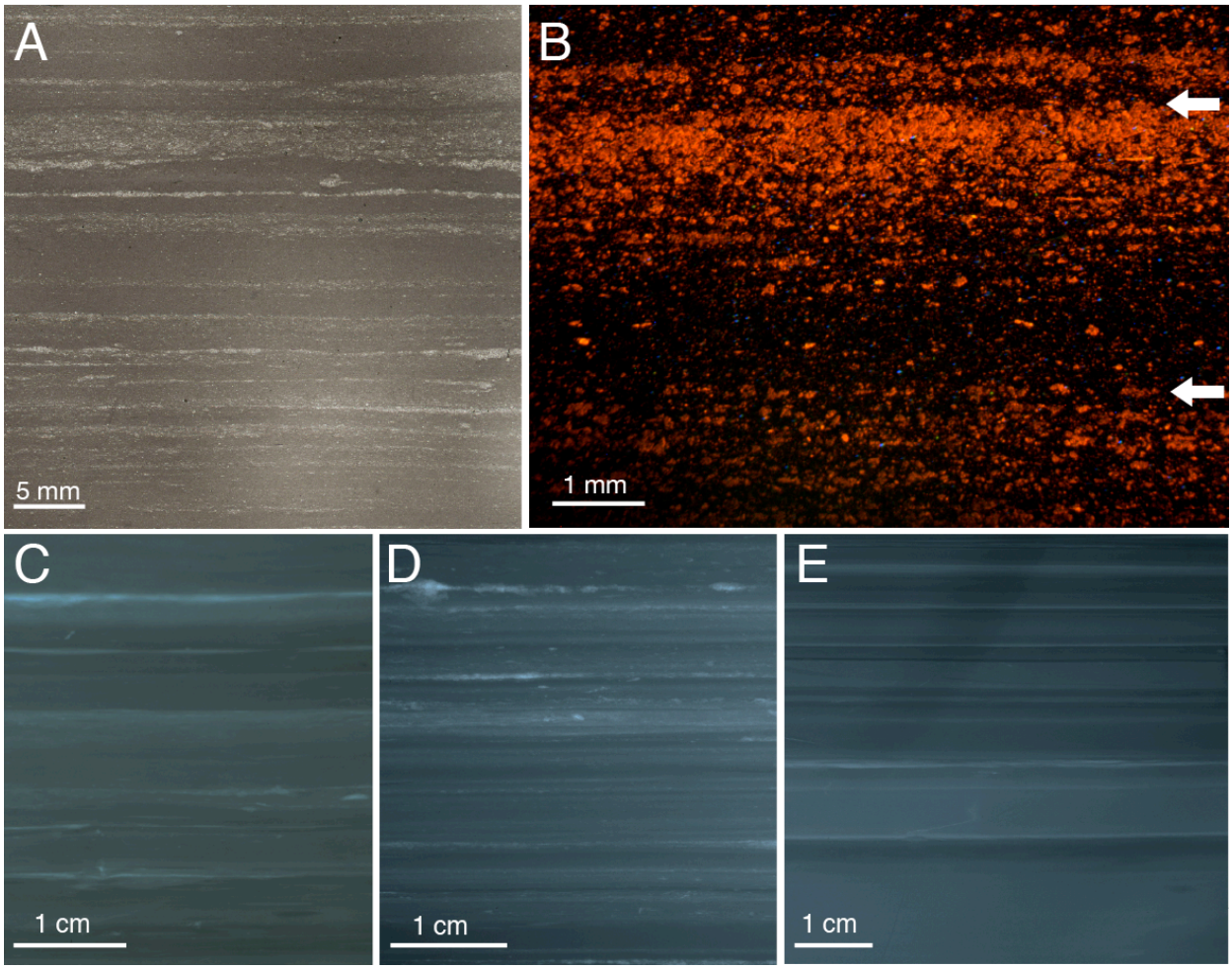


**Figure S3:** Thin section micrographs (A, B) and X-radiographs of slab samples (C-E), illustrating the bed-capping distribution of authigenic carbonate cements in BST-bearing claystones. (A) Thin section of Marjum Formation shown in transmitted light. Carbonate cements at bed tops appear bright, clay-rich bed bases appear gray. (B) Cathodoluminescence micrograph of thin section of BST interval of Kaili Formation, arrows mark base (lower) and top (upper) of a typical BST-bearing claystone lamina, 3mm in thickness. Carbonates, which exhibit bright orange luminesce, are concentrated at bed tops and become less abundant down bed. The dark, non-luminescent portions of the image are clay-rich with subsidiary carbonate dispersed throughout the claystone fabric. (C-E) X-radiographs of slab samples of BST –bearing claystones. Carbonate-rich portions of event-deposited laminae are less easily penetrated by X-rays and appear bright in X-radiograph, whereas clay-rich portions appear dark in color, revealing concentration of carbonate cements at the tops of individual mm-scale laminae. (C) "thin" Stephen Formation, Stanley Glacier locality. (D) Wheeler Formation, Drum Mountains locality. (E) Marjum Formation, Marjum Pass Locality.

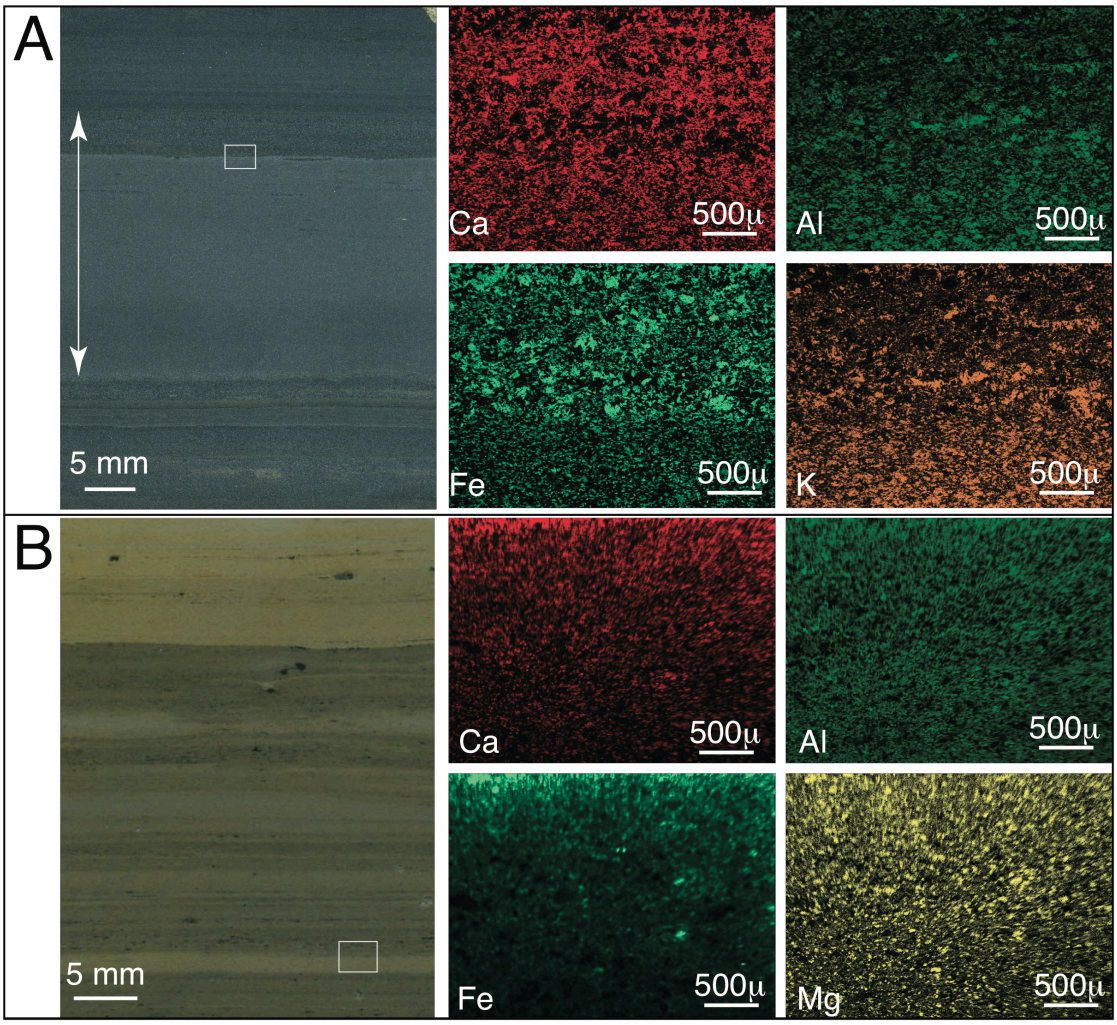


**Figure S4.** Energy Dispersive X-ray Spectroscopy (EDX) elemental maps of bed tops of BST claystones showing concentration of calcium carbonate cements in bed tops, with polished slabs at left showing the locations of the two areas represented in the elemental maps (boxes). In each elemental map, brightness corresponds to elemental abundance. (A) Burgess Shale, Walcott Quarry Member, Great *Eldoniia* Layer (GEL). Elemental maps of Ca and Fe reveal concentration of calcite and pyrite at the bed top, coincident with decreases in Al and K, which reside in clay minerals. Al and K are concentrated lower in the bed, indicating an increasing proportion of clay relative to calcium carbonate, as also shown in Figure 2. Arrow indicates vertical extent of the GEL. (B) BST-bearing interval of the Wheeler Formation, Drum Mountains locality. Elemental maps of Ca and Mg indicate concentration of magnesian calcite at bed top. Some Mg also resides in clay minerals, and as a result, Ca and Mg do not share the same precise distribution in the sample. Elemental map of Fe indicates concentration of pyrite at bed top, coincident with a decrease in Al, which resides in clay minerals, indicating an increasing proportion of clay minerals relative to calcium carbonate down the bed.

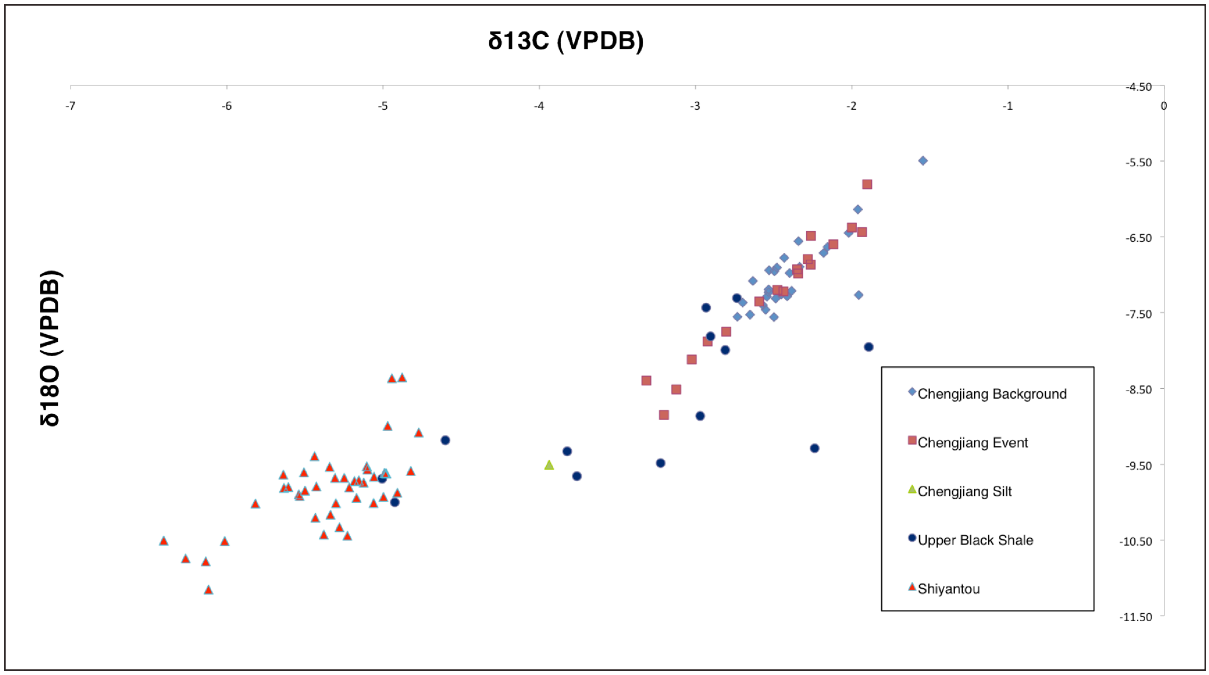


**Figure S5.** Plot of $\delta^{13}C$ vs. $\delta^{18}O$ of 103 analyses of carbonate cements from the Haikou core, including the Chengjiang interval, and the underlying "Upper Black Shale" and Shiyantou Formations. The two clusters of data apparent on the plot comprise fields of early vs. late diagenetic cements. Shiyantou Fm. cements contain isotopic values typical of diageneitc carbonate cements in fine-grained siliciclastics. They are characterized by more negative $\delta^{13}C$ and $\delta^{18}O$ values, indicating significant input of organodiagentically derived bicarbonate and higher temperatures of crystallization. In contrast, Chengjiang carbonate cements are characterized by $\delta^{13}C$ values that lie within the range of reported Early Cambrian seawater values (9) and display less negative $\delta^{18}O$ values, indicating early precipitation at lower temperature from a seawater source, with minor organic contribution.

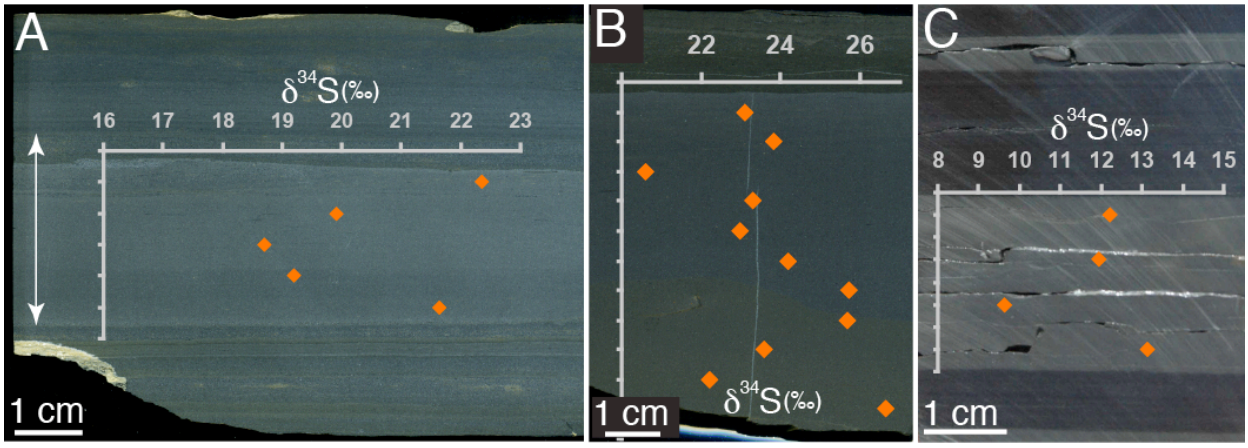


**Figure S6.** Distribution of $\delta^{34}S_{pyrite}$ values across single event-deposited BST-bearing claystone beds in the Walcott Quarry Member of the Burgess Shale (A-B) and the Chengjiang deposit (C). Low fractionation of $\delta^{34}S_{pyrite}$ values from Cambrian seawater $SO_4^{2-}$ values provides clear evidence of $SO_4^{2-}$ limitation within each bed during pyrite precipitation (10) (Fig. 3, Table S1). However, $\delta^{34}S_{pyrite}$ values do not show consistent trends towards heavier values down-bed, as would be expected if $SO_4^{2-}$ limitation within the porewaters was induced by reduced diffusion of $SO_4^{2-}$ into the beds as a result of event-driven deposition alone (11). Therefore, an additional mechanism of $SO_4^{2-}$ limitation during early diagenesis is required. (A) Great *Eldoniia* Layer, Walcott Quarry Member, Burgess Shale Fm. (2.8 cm thick) (B) Great *Marrella* Layer, Walcott Quarry, Burgess Shale Fm. (7.6 cm thick). (C) BST-bearing event bed from the Chengjiang deposit, Haikou core, 23.30m depth (2.1 cm thick). $\delta^{34}S_{pyrite}$ values for additional subsamples taken from cross-bed transects within single event-deposited beds of the Chengjiang deposit are reported in table S1.

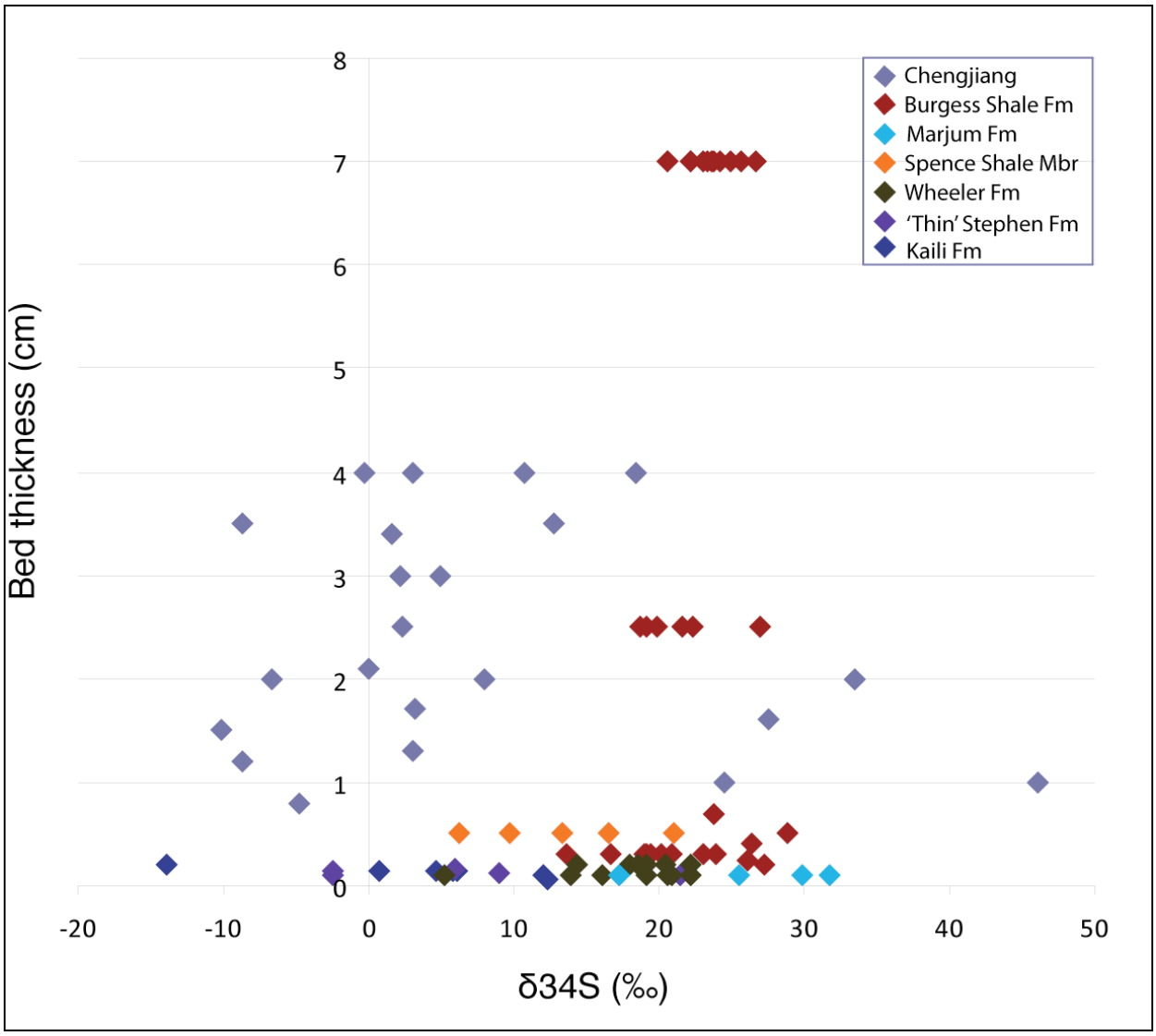


**Figure S7.** Plot of $\delta^{34}S_{pyrite}$ vs. bed thickness for all BST deposits analyzed, showing absence of correlation.

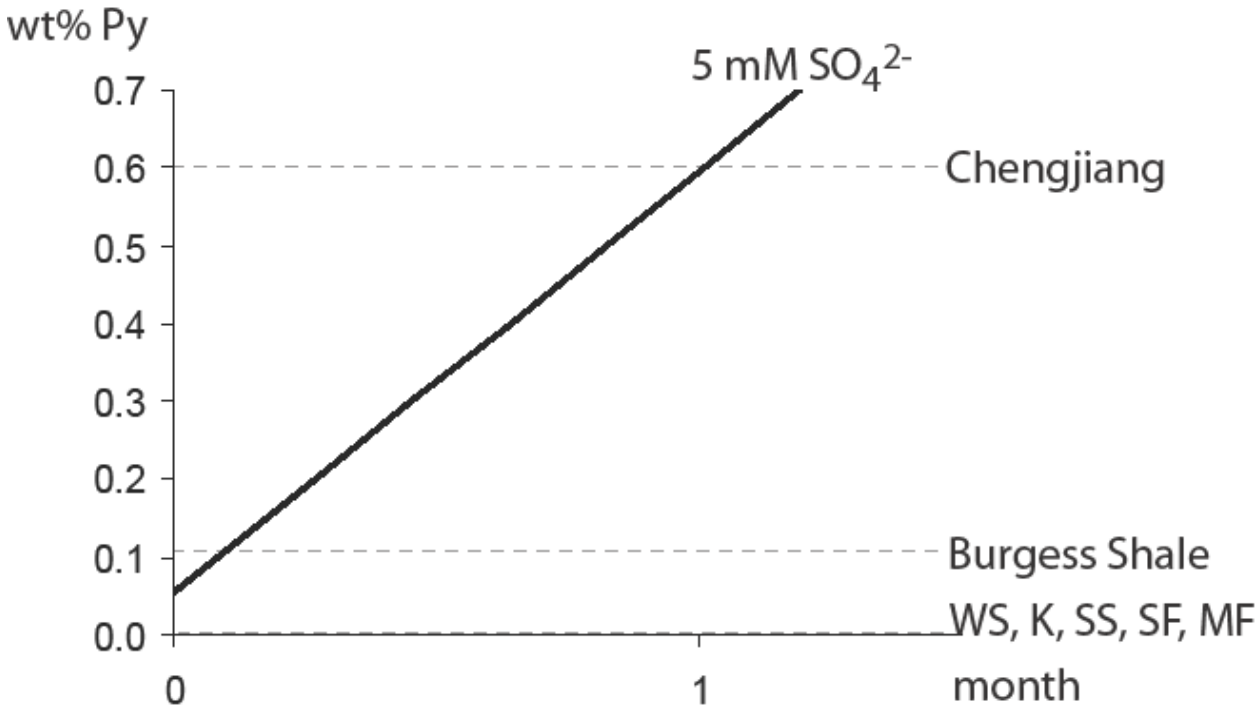


**Figure S8.** Time required to precipitate pyrite contents measured in fossiliferous beds of BST deposits, calculated for a Cambrian oceanic sulfate concentration of 5 mM (12). The vertical flux is calculated as $J(x)=\Phi * Ds * (\partial C/\partial x)$ (13), where porosity ($\Phi$) is 0.7. The diffusion coefficient ($D_s$) for sulfate in sediment is calculated as $D_s= D_{sw}/(1+n(1- \Phi))$, where n=2.7 (14) and $D_{sw}$ for sulfate at 10°C = 0.68e-5 $cm^2/s$ (15). The gradient of sulfate ($\partial C/\partial x$) is set over 10 cm. Under this simple approximation, the average pyrite content of fossil-bearing beds from Chengjiang (dashed upper grey line) required no longer than 1 month to precipitate, while far less time was required to form the pyrite observed in other BST deposits (Burgess Shale, Wheeler Formation (WS), Kaili (K), Spence Shale (SS), Stephen Fm (SF), Marjum Fm (MF)).

**Table S1.** The isotopic composition of pyrite sulfur from 6 of the principal Burgess Shale-type deposits and from the newly-reported "thin" Stephen Formation of the Canadian Rocky Mountains. Pyrite content is generally low, implying that heavy isotopic composition resulted from restriction of sulfate, as also indicated by low fractionation from Cambrian seawater values. Reduced pyrite content of some samples may have resulted from weathering and/or metamorphism (16, 17).

| Formation | Sample | $\partial^{34}S$ (‰) | Pyrite (wt%) | Bed type | Comments |
|---|---|---|---|---|---|
| **Chengjiang deposit** | | | | | |
| | 12.96 | 24.5 | 0.30 | single BST event bed | Borehole Sample, Haikou Core |
| | 12.96E | 17.9 | 0.11 | BST event bed subsample | Bed Top, Borehole Sample, Haikou Core |
| | 12.96D | 18.7 | 0.04 | BST event bed subsample | Bed Base, Borehole Sample, Haikou Core |
| | 12.96C | 22.2 | 0.22 | BST event bed subsample | Bed Top, Borehole Sample, Haikou Core |
| | 12.96B | 34.1 | 0.33 | BST event bed subsample | Bed Middle, Borehole Sample, Haikou Core |
| | 12.96A | 33.4 | 0.34 | BST event bed subsample | Bed Base, Borehole Sample, Haikou Core |
| | 13.00 | -10.7 | 0.47 | background interval | Borehole Sample, Haikou Core |
| | 14.40 | -9.0 | 0.01 | background interval | Borehole Sample, Haikou Core |
| | 15.18 | -9.6 | 0.40 | background interval | Borehole Sample, Haikou Core |
| | 15.2 | 33.5 | 0.27 | single BST event bed | Borehole Sample, Haikou Core |
| | 15.20C | 30.1 | 0.08 | BST event bed subsample | Bed Top, Borehole Sample, Haikou Core |
| | 15.20B | 33.1 | 0.22 | BST event bed subsample | Bed Middle, Borehole Sample, Haikou Core |
| | 15.20A | 40.8 | 0.36 | BST event bed subsample | Sample Base, Borehole Sample, Haikou Core |
| | 15.26 | 46.1 | 0.29 | single BST event bed | Borehole Sample, Haikou Core |
| | 15.28 | 6.3 | 0.58 | background interval | Borehole Sample, Haikou Core |
| | 16.73 | 2.7 | 0.26 | background interval | Borehole Sample, Haikou Core |
| | 16.75 | 2.3 | 0.00 | single BST event bed | Borehole Sample, Haikou Core |
| | 17.2 | -10.3 | 0.73 | single BST event bed | Borehole Sample, Haikou Core |
| | 17.25 | 7.2 | 0.89 | single BST event bed | Borehole Sample, Haikou Core |
| | 19.54 | -8.7 | 0.72 | background interval | Borehole Sample, Haikou Core |
| | 20.09 | -4.8 | 0.47 | single BST event bed | Borehole Sample, Haikou Core |
| | 20.10 | -12.3 | 0.92 | background interval | Borehole Sample, Haikou Core |
| | 20.14 | -0.4 | 0.51 | single BST event bed | Borehole Sample, Haikou Core |
| | 20.15 | -9.3 | 1.01 | background interval | Borehole Sample, Haikou Core |
| | 20.19 | 3.1 | 0.52 | single BST event bed | Borehole Sample, Haikou Core |
| | 20.21 | -11.2 | 0.83 | background interval | Borehole Sample, Haikou Core |
| | 21.27 | -5.7 | 0.66 | background interval | Borehole Sample, Haikou Core |
| | 22.25 | -4.0 | 0.71 | background interval | Borehole Sample, Haikou Core |
| | 23.30 | 2.1 | 0.48 | single BST event bed | Borehole Sample, Haikou Core |
| | 23.30D | 1.7 | 0.64 | BST event bed subsample | Bed Top, Borehole Sample, Haikou Core |
| | 23.30C | 3.7 | 0.60 | BST event bed subsample | Bed Middle, Borehole Sample, Haikou Core |
| | 23.30B | 5.0 | 0.85 | BST event bed subsample | Bed Middle, Borehole Sample, Haikou Core |
| | 23.30A | 9.4 | 0.58 | BST event bed subsample | Bed Base, Borehole Sample, Haikou Core |
| | 23.33 | -7.0 | 0.56 | background interval | Borehole Sample, Haikou Core |
| | 23.37 | -7.8 | 0.80 | background interval | Borehole Sample, Haikou Core |
| | 23.40 | 12.7 | 0.63 | single BST event bed | Borehole Sample, Haikou Core |
| | 23.40D | 12.2 | 1.32 | BST event bed subsample | Bed Top, Borehole Sample, Haikou Core |
| | 23.40C | 11.9 | 0.90 | BST event bed subsample | Bed Middle, Borehole Sample, Haikou Core |
| | 23.40B | 9.6 | 0.89 | BST event bed subsample | Bed Middle, Borehole Sample, Haikou Core |
| | 23.40A | 13.1 | 0.74 | BST event bed subsample | Sample Base, Borehole Sample, Haikou Core |
| | 23.43 | 0.0 | 0.72 | single BST event bed | Borehole Sample, Haikou Core |
| | 23.44 | -8.2 | 0.91 | background interval | Borehole Sample, Haikou Core |
| | 23.46 | 3.1 | 0.74 | single BST event bed | Borehole Sample, Haikou Core |
| | 23.50 | -2.7 | 0.99 | background interval | Borehole Sample, Haikou Core |
| | 23.51 | 27.5 | 0.58 | single BST event bed | Borehole Sample, Haikou Core |
| | 23.52 | 10.7 | 1.10 | single BST event bed | Borehole Sample, Haikou Core |
| | 23.57 | 4.9 | 0.83 | single BST event bed | Borehole Sample, Haikou Core |
| | 23.60 | -9.7 | 0.77 | background interval | Borehole Sample, Haikou Core |
| | 23.91 | -8.3 | 0.99 | background interval | Borehole Sample, Haikou Core |
| | 24.12 | -5.5 | 0.72 | background interval | Borehole Sample, Haikou Core |
| | 24.22 | -4.7 | 0.78 | background interval | Borehole Sample, Haikou Core |
| | 24.62 | -6.0 | 0.90 | background interval | Borehole Sample, Haikou Core |
| | 24.69 | 0.8 | 0.96 | single BST event bed | Borehole Sample, Haikou Core |
| | 24.70 | -4.5 | 0.87 | background interval | Borehole Sample, Haikou Core |
| | 24.76 | -6.7 | 0.76 | background interval | Borehole Sample, Haikou Core |
| | 24.85 | -7.0 | 0.81 | background interval | Borehole Sample, Haikou Core |
| | 24.86 | -8.0 | 1.05 | background interval | Borehole Sample, Haikou Core |
| | 24.91 | -8.9 | 0.76 | background interval | Borehole Sample, Haikou Core |
| | 25.00 | -6.3 | 0.81 | background interval | Borehole Sample, Haikou Core |
| | 25.08 | -6.6 | 0.70 | single BST event bed | Borehole Sample, Haikou Core |
| | 25.10 | 8.0 | 0.69 | single BST event bed | Borehole Sample, Haikou Core |

| | | | | | |
|---|---|---|---|---|---|
| | 25.11 | 1.0 | 1.29 | background interval | Borehole Sample, Haikou Core |
| | 25.14 | -5.9 | 0.87 | background interval | Borehole Sample, Haikou Core |
| | 25.46 | -8.7 | 0.88 | single BST event bed | Borehole Sample, Haikou Core |
| | 25.47 | -8.1 | 1.04 | background interval | Borehole Sample, Haikou Core |
| | 25.48 | -8.7 | 1.03 | single BST event bed | Borehole Sample, Haikou Core |
| | 25.50 | -4.3 | 0.07 | background interval | Borehole Sample, Haikou Core |
| | 25.55 | -10.1 | 1.11 | single BST event bed | Borehole Sample, Haikou Core |
| | 25.55D | -6.6 | 0.73 | BST event bed subsample | Sample Top, Borehole Sample, Haikou Core |
| | 25.55C | 5.6 | 0.04 | BST event bed subsample | Bed Middle, Borehole Sample, Haikou Core |
| | 25.55B | -2.1 | 0.02 | BST event bed subsample | Bed Middle, Borehole Sample, Haikou Core |
| | 25.55A | 7.0 | 0.02 | BST event bed subsample | Sample Base, Borehole Sample, Haikou Core |
| | 25.56 | -5.6 | 0.89 | background interval | Borehole Sample, Haikou Core |
| | 25.60 | 18.4 | 0.91 | single BST event bed | Borehole Sample, Haikou Core |
| | 25.60D | 14.6 | 1.07 | BST event bed subsample | Sample Top, Borehole Sample, Haikou Core |
| | 25.60C | 17.9 | 0.97 | BST event bed subsample | Bed Middle, Borehole Sample, Haikou Core |
| | 25.60B | 20.8 | 0.92 | BST event bed subsample | Bed Middle, Borehole Sample, Haikou Core |
| | 25.60A | 24.7 | 0.81 | BST event bed subsample | Bed Base, Borehole Sample, Haikou Core |
| | 25.61 | 0.9 | 1.05 | background interval | Borehole Sample, Haikou Core |
| | 25.62 | -6.9 | 0.81 | background interval | Borehole Sample, Haikou Core |
| | 25.69 | -8.0 | 0.78 | background interval | Borehole Sample, Haikou Core |
| | 25.72 | 3.1 | 0.52 | single BST event bed | Borehole Sample, Haikou Core |
| | 25.73 | -7.0 | 0.74 | background interval | Borehole Sample, Haikou Core |
| | 25.75 | -4.6 | 0.92 | background interval | Borehole Sample, Haikou Core |
| | 25.92 | -4.1 | 0.88 | background interval | Borehole Sample, Haikou Core |
| | 26.33 | 1.6 | 0.03 | single BST event bed | Borehole Sample, Haikou Core |
| | 26.35 | -10.1 | 0.64 | background interval | Borehole Sample, Haikou Core |
| | 26.61 | -4.0 | 0.00 | background interval | Borehole Sample, Haikou Core |
| | 27.76 | -3.3 | 0.00 | background interval | Borehole Sample, Haikou Core |
| | 28.55 | -3.3 | 0.04 | background interval | Borehole Sample, Haikou Core |
| **Kaili Fm.** | | | | | |
| | CKW 16 | 12.0 | <0.00001 | BST event beds | Wuliu-Zengjaya Section, 16 m above base of Fm. |
| | CKW 50 | 12.3 | <0.00001 | BST event beds | Wuliu-Zengjaya Section, 50 m above base of Fm. |
| | CKM 58 | 5.9 | <0.00001 | BST event beds | Miaobanpo Section, 58 m above base of Fm. |
| | CKM 77 | 4.6 | <0.00001 | BST event beds | Miaobanpo Section, 77m above base of Fm. |
| | CKM 95 | -13.9 | <0.00001 | BST event beds | Miaobanpo Section, 95 m above baseof Fm. |
| | CKM 104 | 0.7 | <0.00001 | BST event beds | Miaobanpo Section,104 m above base of Fm. |
| | CKM 120 | 6.0 | <0.00001 | BST event beds | Miaobanpo Section,120 m above base of Fm. |
| **Spence Shale Mbr.** | | | | | |
| | MH5 0.30 | 13.3 | <0.00001 | BST event beds | Miner's Hollow, Cycle 5 |
| | MH5 0.38 | 6.3 | <0.00001 | BST event beds | Miner's Hollow, Cycle 5 |
| | MH5 0.62 | 9.7 | <0.00001 | BST event beds | Miner's Hollow, Cycle 5 |
| | MH5 0.95 | 16.5 | <0.00001 | BST event beds | Miner's Hollow, Cycle 5 |
| | MH5 1.21 | 21.0 | <0.00001 | BST event beds | Miner's Hollow, Cycle 5 |
| **Burgess Shale Fm.** | | | | | |
| | WQ7 120 GEL | 27.0 | 0.14 | BST event beds | Walcott Quarry Member, Great Eldoniia Layer |
| | WQ6 0 GML | 25.0 | 0.30 | BST event beds | Walcott Quarry Member, Great Marrella Layer (GML) |
| | WQ5 -120 | 27.3 | 0.16 | BST event beds | Walcott Quarry Member, 120 cm below GML |
| | WQ4 -130 | 28.8 | 0.23 | BST event beds | Walcott Quarry Member, 130 cm below GML |
| | WQ3 -210 | 26.1 | 0.23 | BST event beds | Walcott Quarry Member, 210 cm below GML |
| | WQ2 -250 | 26.4 | 0.05 | BST event beds | Walcott Quarry Member, 250 cm below GML |
| | WQ1 -400 | 23.8 | 0.01 | BST event beds | Walcott Quarry Member, 400 cm below GML |
| | GEL-A | 21.6 | 0.16 | BST event bed subsample | Walcott Quarry Member, Great Eldoniia Layer; Bed Base |
| | GEL-B | 19.2 | 0.08 | BST event bed subsample | Walcott Quarry Member, Great Eldoniia Layer |
| | GEL-C | 18.7 | 0.10 | BST event bed subsample | Walcott Quarry Member, Great Eldoniia Layer |
| | GEL-D | 19.9 | 0.10 | BST event bed subsample | Walcott Quarry Member, Great Eldoniia Layer |
| | GEL-E | 22.4 | 0.15 | BST event bed subsample | Walcott Quarry Member, Great Eldoniia Layer; Bed Top |
| | GML-A | 26.6 | 0.02 | BST event bed subsample | Walcott Quarry Member, Great Marrella Layer; Bed Base |
| | GML-B | 22.2 | 0.01 | BST event bed subsample | Walcott Quarry Member, Great Marrella Layer |
| | GML-C | 23.6 | 0.02 | BST event bed subsample | Walcott Quarry Member, Great Marrella Layer |
| | GML-D | 25.7 | 0.03 | BST event bed subsample | Walcott Quarry Member, Great Marrella Layer |
| | GML-E | 25.7 | 0.02 | BST event bed subsample | Walcott Quarry Member, Great Marrella Layer |
| | GML-F | 24.2 | 0.03 | BST event bed subsample | Walcott Quarry Member, Great Marrella Layer |
| | GML-G | 23.0 | 0.02 | BST event bed subsample | Walcott Quarry Member, Great Marrella Layer |
| | GML-H | 23.3 | 0.04 | BST event bed subsample | Walcott Quarry Member, Great Marrella Layer |
| | GML-I | 20.6 | 0.05 | BST event bed subsample | Walcott Quarry Member, Great Marrella Layer |
| | GML-K | 23.8 | 0.08 | BST event bed subsample | Walcott Quarry Member, Great Marrella Layer |
| | GML-L | 23.1 | 0.03 | BST event bed subsample | Walcott Quarry Member, Great Marrella Layer; Bed Top |
| | RQ1 | 23.0 | 0.05 | BST event beds | Raymond Quarry Member |
| | RQ2 | 20.1 | 0.11 | BST event beds | Raymond Quarry Member |
| | RQ3 | 20.9 | 0.13 | BST event beds | Raymond Quarry Member |
| | RQ4 | 23.9 | 0.10 | BST event beds | Raymond Quarry Member |
| | RQ5 | 19.1 | 0.20 | BST event beds | Raymond Quarry Member |
| | RQ6 | 19.4 | 0.19 | BST event beds | Raymond Quarry Member |
| | RQ7 | 13.6 | 0.07 | BST event beds | Raymond Quarry Member |

| | | | | | |
|---|---|---|---|---|---|
| | RQ8 | 19.0 | 0.15 | BST event beds | Raymond Quarry Member |
| | RQ9 | 16.7 | 0.23 | BST event beds | Raymond Quarry Member |
| **"thin" Stephen Fm.** | | | | | |
| | SG1 27.01 | -2.4 | <0.00001 | BST event beds | Stanley Glacier, Cycle 5, 27.01 m above base |
| | SG1 27.62 | -2.5 | <0.00001 | BST event beds | Stanley Glacier, Cycle 5, 27.62 m above base |
| | SG1 28.37 | 5.9 | <0.00001 | BST event beds | Stanley Glacier, Cycle 5, 28.37 m above base |
| | SG1 29.65 | 9.0 | <0.00001 | BST event beds | Stanley Glacier, Cycle 5, 29.65 m above base |
| | SG1 30.00 | 21.4 | <0.00001 | BST event beds | Stanley Glacier, Cycle 5, 30.00 m above base |
| **Wheeler Fm.** | | | | | |
| | SSv 17-19 | 5.3 | 0.05 | BST event beds | Lower Wheeler, Swasey Spring |
| | SSv 27.5-29.5 | 16.1 | 0.04 | BST event beds | Lower Wheeler, Swasey Spring |
| | SSv 29.5-30.5 | 22.1 | 0.03 | BST event beds | Lower Wheeler, Swasey Spring |
| | SSv 40-41 | 20.9 | 0.04 | BST event beds | Lower Wheeler, Swasey Spring |
| | SSv 41-42 | 20.5 | 0.01 | BST event beds | Lower Wheeler, Swasey Spring |
| | SSa 1.63-1.64 | 13.9 | 0.01 | BST event beds | Lower Wheeler, Swasey Spring |
| | SSa 1.74-1.76 | 19.1 | 0.01 | BST event beds | Lower Wheeler, Swasey Spring |
| | SSa 1.87-1.88 | 20.6 | 0.02 | BST event beds | Lower Wheeler, Swasey Spring |
| | DM j 1.2-2.0 | 19.1 | 0.02 | BST event beds | Upper Wheeler, Drum Mtns. |
| | DM j 5.5-6.5 | 19.2 | 0.02 | BST event beds | Upper Wheeler, Drum Mtns. |
| | DM j 13.0-14.5 | 17.9 | 0.04 | BST event beds | Upper Wheeler, Drum Mtns. |
| | DM j 19.5-20.5 | 18.5 | 0.03 | BST event beds | Upper Wheeler, Drum Mtns. |
| | DM j 21.0-22.0 | 22.2 | 0.02 | BST event beds | Upper Wheeler, Drum Mtns. |
| | DM j 28.0-29.0 | 20.5 | 0.01 | BST event beds | Upper Wheeler, Drum Mtns. |
| | DM j 35.0-36.0 | 14.3 | 0.01 | BST event beds | Upper Wheeler, Drum Mtns. |
| **Marjum Fm.** | | | | | |
| | MJ 0.01 | 25.5 | <0.00001 | BST event beds | Lower Marjum, Sponge Gulch |
| | MJ 0.13 | 17.3 | <0.00001 | BST event beds | Lower Marjum, Sponge Gulch |
| | MJ 0.21 | 29.9 | <0.00001 | BST event beds | Lower Marjum, Sponge Gulch |
| | MJ 0.47 | 29.9 | <0.00001 | BST event beds | Lower Marjum, Sponge Gulch |
| | MJ 0.68 | 31.8 | <0.00001 | BST event beds | Lower Marjum, Sponge Gulch |

**Table S2.** $\delta^{13}C$ vs. $\delta^{18}O$ of carbonate cements of BST-bearing claystones. Data from Chengiang are given in Figure SI5; data from all other formations analyzed are given below.

| Sample | d13C(VPDB) | d18O(VPDB) | Sample type | Locality |
|---|---|---|---|---|
| **Kaili Fm.** | | | | |
| CK 34 | -0.36 | -8.09 | BST event beds | Miaobanpo Quarry |
| CK ELD-1 | -2.53 | -9.20 | BST event beds | Miaobanpo Quarry |
| CK-A | -1.00 | -7.13 | BST event beds | Miaobanpo Quarry |
| **Spence Shale Mbr.** | | | | |
| MH5 118 | -0.73 | -15.25 | BST event beds | Cycle 5, Miner's Holow |
| MH5 126 | -1.59 | -10.49 | BST event beds | Cycle 5, Miner's Holow |
| CS ON | 0.11 | -15.12 | BST event beds | Lower Spence Mbr., Oneida Narrows |
| **Burgess Shale Fm.** | | | | |
| BPB | -0.20 | -14.61 | BST event beds | Walcott Quarry, Greater Phyllopod Bed |
| OG4 | -0.09 | -13.96 | BST event beds | Mt. Stephen Trilobite Beds, BST event beds |
| GPB 124 | -0.29 | -14.27 | BST event beds | Walcott Quarry, Greater Phyllopod Bed |
| GPB 125 | -0.05 | -14.55 | single BST event bed | Walcott Quarry, Great Eldoniia Layer |
| OG4 | -0.09 | -13.96 | BST event beds | Mt. Stephen Trilobite Beds, BST event beds |
| **"thin' Stephen Fm.** | | | | |
| BSG 1033 | -0.90 | -11.38 | BST event beds | Stanley Glacier, Cycle 5 |
| BSG 1035 | 0.32 | -8.91 | BST event beds | Stanley Glacier, Cycle 5 |
| SG1 27.01 | -2.11 | -15.71 | BST event beds | Stanley Glacier, Cycle 5 |
| SG1 27.62 | -1.91 | -12.82 | BST event beds | Stanley Glacier, Cycle 5 |
| SG1 28.37 | -1.75 | -12.85 | BST event beds | Stanley Glacier, Cycle 5 |
| SG1 29.65 | -2.23 | -13.21 | BST event beds | Stanley Glacier, Cycle 5 |
| SG1 30.0 | -1.76 | -13.16 | BST event beds | Stanley Glacier, Cycle 5 |
| **Wheeler Fm.** | | | | |
| DM311 | -0.15 | -10.19 | BST event beds | Upper Wheeler Fm., Drum Mountains |
| DMJ16 | -0.11 | -9.82 | BST event beds | Upper Wheeler Fm., Drum Mountains |
| DMJ17 | -0.14 | -10.02 | BST event beds | Upper Wheeler Fm., Drum Mountains |
| DMJ20 | -0.15 | -10.01 | BST event beds | Upper Wheeler Fm., Drum Mountains |
| DMJ28 | -0.20 | -10.43 | BST event beds | Upper Wheeler Fm., Drum Mountains |
| DMJ31 | -0.17 | -9.73 | BST event beds | Upper Wheeler Fm., Drum Mountains |
| DMJ34 | -0.18 | -10.51 | BST event beds | Upper Wheeler Fm., Drum Mountains |
| DMJ36-38 | -0.24 | -10.65 | BST event beds | Upper Wheeler Fm., Drum Mountains |
| DMJ5 | -0.10 | -9.63 | BST event beds | Upper Wheeler Fm., Drum Mountains |
| DMJ60 | -0.48 | -11.45 | BST event beds | Upper Wheeler Fm., Drum Mountains |
| DMM2 | 0.80 | -8.98 | BST event beds | Upper Wheeler Fm., Drum Mountains |
| DMUA | -0.56 | -9.42 | BST event beds | Upper Wheeler Fm., Drum Mountains |
| DMUB | -0.05 | -9.08 | BST event beds | Upper Wheeler Fm., Drum Mountains |
| SS1 | -0.85 | -9.75 | BST event beds | Lower Wheeler Fm., Swasey Spring |
| SS2 | -0.79 | -9.87 | BST event beds | Lower Wheeler Fm., Swasey Spring |
| SS3 | -0.80 | -9.78 | BST event beds | Lower Wheeler Fm., Swasey Spring |
| WA1 0.07 | -0.43 | -9.31 | BST event beds | Upper Wheeler Fm., Wheeler Amphiteater |
| WA1 0.10 | -0.92 | -9.94 | BST event beds | Upper Wheeler Fm., Wheeler Amphiteater |
| WA1 0.37 | -0.85 | -9.39 | BST event beds | Upper Wheeler Fm., Wheeler Amphiteater |
| WA1 0.49T | -0.31 | -9.84 | BST event beds | Upper Wheeler Fm., Wheeler Amphiteater |
| WA1 0.96 | -0.73 | -9.54 | BST event beds | Upper Wheeler Fm., Wheeler Amphiteater |

| | | | | |
|---|---|---|---|---|
| WA1 1.39T | -0.47 | -10.04 | BST event beds | Upper Wheeler Fm., Wheeler Amphiteater |
| WA2 2.09 | -0.97 | -10.48 | BST event beds | Middle Wheeler Fm., Wheeler Amphiteater |
| WA2 2.11 | -0.78 | -10.68 | BST event beds | Middle Wheeler Fm., Wheeler Amphiteater |
| WA2 3.46 | -1.20 | -10.48 | BST event beds | Middle Wheeler Fm., Wheeler Amphiteater |
| WA2-2 0.0 | -1.95 | -12.17 | BST event beds | Middle Wheeler Fm., Wheeler Amphiteater |
| WA2-2 0.1 | -1.13 | -10.75 | BST event beds | Middle Wheeler Fm., Wheeler Amphiteater |
| WA2-2 0.9 | -1.10 | -10.82 | BST event beds | Middle Wheeler Fm., Wheeler Amphiteater |
| WA2-2 1.5 | -1.65 | -12.78 | BST event beds | Middle Wheeler Fm., Wheeler Amphiteater |
| WA2-2 1.6 | -1.49 | -11.53 | BST event beds | Middle Wheeler Fm., Wheeler Amphiteater |
| | | | | |
| **Marjum/Pierson Cove Fm.** | | | | |
| WHQ | -0.17 | -10.14 | BST event beds | Upper Marjum Fm., Marjum Pass |
| MP | 0.03 | -10.05 | BST event beds | Upper Marjum Fm., Marjum Pass |
| MJ KK | 0.77 | -8.72 | BST event beds | Lower Marjum Fm., Kell's Knolls |
| RW | 0.83 | -8.94 | BST event beds | Lower Marjum Fm., Red Cliffs Wash |
| SG1 | 0.07 | -10.33 | BST event beds | Lower Marjum Fm., Sponge Gully |
| SG2 | 0.22 | -10.40 | BST event beds | Lower Marjum Fm., Sponge Gully |
| MJ1 | 0.31 | -10.30 | BST event beds | Lower Marjum Fm., Sponge Gully |
| MJ13 | 0.26 | -10.42 | BST event beds | Lower Marjum Fm., Sponge Gully |
| MJ21 | 0.30 | -10.34 | BST event beds | Lower Marjum Fm., Sponge Gully |
| MJ47 | 0.24 | -10.40 | BST event beds | Lower Marjum Fm., Sponge Gully |
| MJ68 | 0.47 | -10.43 | BST event beds | Lower Marjum Fm., Sponge Gully |
| DMQ 45 | -0.60 | -10.24 | BST event beds | Lower Pierson Cove Fm., Drum Mountains |
| DMQ 61 | -0.76 | -10.16 | BST event beds | Lower Pierson Cove Fm., Drum Mountains |
| DMQ 70 | -0.68 | -10.40 | BST event beds | Lower Pierson Cove Fm., Drum Mountains |
| DMQ1 | -0.72 | -7.80 | BST event beds | Lower Pierson Cove Fm., Drum Mountains |
| DMQ2 | -0.52 | -10.64 | BST event beds | Lower Pierson Cove Fm., Drum Mountains |
| DMQ3 | -0.46 | -10.22 | BST event beds | Lower Pierson Cove Fm., Drum Mountains |
| DMQ4 | -0.53 | -10.35 | BST event beds | Lower Pierson Cove Fm., Drum Mountains |
| DMQ5 | -0.47 | -10.28 | BST event beds | Lower Pierson Cove Fm., Drum Mountains |
| DMQ6 | -0.51 | -10.13 | BST event beds | Lower Pierson Cove Fm., Drum Mountains |
| DMQ7 | -0.53 | -10.23 | BST event beds | Lower Pierson Cove Fm., Drum Mountains |
| DMQ8 | -0.51 | -10.27 | BST event beds | Lower Pierson Cove Fm., Drum Mountains |

**References**


1. Conway Morris S (1997) *The Crucible of Creation: the Burgess Shale and the Rise of Animals* (Oxford University Press) p 272.
2. Caron J-B, Gaines RR, Mángano MG, Streng M, & Daley AC (2010) A new Burgess Shale–type assemblage from the "thin" Stephen Formation of the southern Canadian Rockies *Geology* 38(9):811-814.
3. Hou X-G, Aldridge RJ, Bergström J, Siveter DJ, & Feng X-H (2004 ) *The Cambrian fossils of Chengjiang, China* (Blackwell Science Ltd., Oxford, UK).
4. Briggs DEG, Erwin DH, & Collier FJ (1994) *The Fossils of the Burgess Shale* p 238
5. Butterfield NJ (1994) Burgess Shale-type fossils from a Lower Cambrian shallow-shelf sequence in Northerwestern Canada. *Nature* 369:477-479.
6. SHAW AB (1958) Stratigraphy and structure of the St. Albans area, northwestern Vermont. . *Society of America Bulletin* 69:519-568.
7. Budd GE & Peel JS (1998) A new xenusiid lobopod from the early Cambrian Sirius Passet fauna of North Greenland. *Palaeontology* 41:1201-1213.
8. O'Brien NR, Nakazawa K, & Tokuhashi S (1980) Use of clay fabric to distinguish turbiditic and hemipelagic siltstones and silts. *Sedimentology* 27(1):47-61.
9. Montanez IP, Osleger DA, Banner J, Mack LE, & Musgrove M (2000) Evolution of the Sr and C isotope composition of Cambrian Oceans. . *GSA today* 10:1-7.
10. Habicht KS, Gade M, Thamdrup B, Berg P, & Canfield DE (2002) Calibration of sulfate levels in the Archean ocean. *Science* 298:2372-2374.
11. Canfield DE, Raiswell R, & Bottrell S (1992) The reactivity of sedimentary iron minarals toward sulfide. *Am. J. Sci.* 292:659-683.
12. Lowenstein TK, Hardie LA, Timofeff MN, & Demicco RV (2003) Secular variation in seawater chemistry and the origin of calcium chloride basinal brines. *Geology* 31:857-860.
13. Westrich JT & R.A. B (1984) The role of sedimentary organic matter in bacterial sulfate reduction: the *G* model tested. *Limnol. Oceanogr.* 29:236-249.
14. Iversen N & Jørgensen BB (1993) Diffusion Coefficients of Sulfate and Methane in Marine Sediments: Influence of porosity. *Geochim. Cosmochim. Acta* 57:571-578.
15. Boudreau BP (1997) *Diagenetic Models and Their Implementation.* (Springer, New York) p 414 pp.
16. Powell WG (2003) Greenschist-facies metamorphism of the Burgess Shale and its implications for models of fossil formation and preservation. *Can. J. Earth Sci.* 40(10):13-25.
17. Gabbott SE, Hou XG, Norry MJ, & Siveter DJ (2004) Preservation of Early Cambrian animals of the Chengjiang biota. *Geology* 32(10):901-904.